UDC 621.315.592:621.317
DOI: 10.15587/1729-4061.2026.353016

DESIGN OF AN AUTOMATIC SYSTEM FOR MONITORING THE TECHNICAL CONDITION OF FIBER-OPTIC CABLES

Aliya Alkina
Candidate of Technical Sciences, Senior Lecturer*
ORCID: https://orcid.org/0000-0003-4879-0593

Ali Mekhtiyev
Candidate of Technical Sciences, Professor,
Vice-Rector for Science and Innovation**
ORCID: https://orcid.org/0000-0002-2633-3976

Yelena Neshina
Corresponding author
Candidate of Technical Sciences, Associate Professor, Head of Department*
E-mail: e.neshina@ktu.edu.kz
ORCID: https://orcid.org/0000-0002-8973-2958

Adam Ujma
PhD, Associate Professor
Faculty of Technical Sciences
University of Applied Sciences in Nysa
Obrońców Tobruku str., 5, Nysa, Poland, 48-300
ORCID: https://orcid.org/0000-0001-5331-6808

Ruslan Mekhtiyev
Doctoral Student PhD
Department of Automation and Production Processes**
ORCID: https://orcid.org/0000-0001-5416-3444

Madiyar Musagazhinov
Doctoral Student PhD
Department of Electrical Equipment Operation
S. Seifullin Kazakh Agrotechnical Research University
Zhenis ave., 62, Astana, Republic of Kazakhstan, 010000
ORCID: https://orcid.org/0000-0002-4521-8172

Yekaterina Bilichenko
Master of Optical Engineering, Senior Lecturer*
ORCID: https://orcid.org/0000-0001-5709-3576

*Department of Power Systems**
**Abylkas Saginov Karaganda Technical University
N. Nazarbayev ave., 56, Karaganda, Republic of Kazakhstan, 100000

This study examines the process of monitoring the technical condition of fiber-optic cables based on the recording and analysis of changes in the pixel structure of the optical spot formed by cladding radiation under mechanical stress. The task addressed relates to the lack of affordable and easy-to-implement means for continuous monitoring of the integrity of fiber-optic communication lines capable of promptly detecting mechanical stress and unauthorized access attempts.

This paper suggests a monitoring principle based on recording additional optical losses arising from microbending of the optical fiber, followed by image processing on a high-resolution photo matrix. It has been experimentally established that changes in the pixel structure of the optical spot formed by cladding radiation on the surface of the high-resolution photo matrix linearly correlate with the magnitude of the applied load and the level of additional losses.

The results are attributed to the redistribution of optical power between the fiber core and cladding due to the photo-elastic effect. A distinctive feature of the proposed approach is its elimination of interferometric and reflectometric methods and the use of intelligent optical-digital pixel analysis, which reduces system cost, facilitates scalability, and is resistant to interference.

The designed system could be used for continuous monitoring of fiber-optic communication lines, utility lines, as well as long-distance facilities under real-world conditions, with monitored sections up to 60 km long. Laboratory tests confirmed the system's sensitivity to mechanical loads of 5 N and its suitability for integration into existing telecommunications networks

Keywords: fiber-optic cables, micro bends, optical losses, photomatrix, pixel analysis, distributed monitoring

Received 26.11.2025
Received in revised form 19.01.2026
Accepted 11.02.2026
Published 27.02.2026

How to Cite: *Alkina, A., Mekhtiyev, A., Neshina, Y., Ujma, A., Mekhtiyev, R., Musagazhinov, M., Bilichenko, Y. (2026). Design of an automatic system for monitoring the technical condition of fiber-optic cables. Eastern-European Journal of Enterprise Technologies, 1 (5 (139)), 26–42. https://doi.org/10.15587/1729-4061.2026.353016*

1. Introduction

Fiber-optic cables are currently a fundamental element of telecommunications, energy, and industrial infrastructure, enabling the transmission of information over long distances with high reliability and noise immunity. As the length of fiber-optic transmission lines (FOTL) increases and their applications expand, the importance of ensuring their technical integrity, operational safety, and protection from external mechanical influences increases. Damage to optical cables, unauthorized access, and hidden defects lead to information loss, financial losses, and reduced operational reliability of critical facilities.

Copyright © 2026, Authors. This is an open access article under the Creative Commons CC BY license

Despite significant advances in fiber-optic line monitoring methods based on optical reflectometry, interferometry, and fiber Bragg gratings, these approaches are characterized by high cost, complex hardware implementation, and limited applicability in distributed and industrial networks. Furthermore, many existing methods focus primarily on fault localization but do not provide effective monitoring of mechanical influences or early detection of potentially hazardous cable conditions.

In today's environment, the scientific challenge of devising alternative approaches to monitoring the technical condition of fiber-optic cables, based on simple, scalable, and cost-effective methods for recording changes in optical parameters, is particularly pressing. A promising area of research is the study of optical radiation redistribution processes in fiber under mechanical stress, particularly phenomena associated with microbending and additional optical losses, which remain insufficiently studied for their practical use in monitoring systems.

Therefore, research into the principles of monitoring the technical condition of fiber-optic cables based on the analysis of changes in optical radiation parameters under mechanical stress is relevant.

2. Literature review and problem statement

Reviews of distributed fiber-optic sensors in structural monitoring emphasize their effectiveness for monitoring extended structures [1]. These technologies utilize scattering and interferometry to detect deformations in bridges and tunnels, integrating sensors into the structure. However, these solutions are not adapted to communication cables and remain expensive. Furthermore, adapting these methods to fiber-optic communication cables and making them economically feasible for intra-area and intra-industrial networks remain unresolved.

Paper [2] reports the results of a review of distributed fiber-optic sensors for monitoring civil structures. It is shown that integrating fibers into structures enables real-time detection of deformations and cracks. However, unresolved issues remain, including the high cost of equipment and the complexity of calibration, limiting their use in telecommunication networks.

Particular attention is paid to microbending sensors in the context of optical stress sensors. Study [3] reveals the principles and architectures of such devices, highlighting noticeable changes in light intensity under mechanical stress. However, scaling the technology to long cable lines and integrating it into continuous monitoring systems remain unresolved challenges.

Distributed sensors are also actively used for tunnel monitoring. Paper [4] demonstrates that methods based on Brillouin and Rayleigh scattering provide high-accuracy anomaly localization. However, the complexity of the equipment and the need for expensive calibration make them unsuitable for the security and monitoring of communication cables.

The development of distributed acoustic sensing with φ-OTDR is also promising. Study [5] demonstrates that this method successfully classifies vibration effects over significant distances. However, the high cost of laser sources and reflectometers hinders its widespread adoption.

Optical fiber speckle sensing opens up new possibilities in sensor technology. Work [6] emphasizes the high sensitivity of speckle pattern analysis to deformations and vibrations. However, scaling this technology to long-distance communication lines and its application to security applications has not yet been fully realized.

The use of artificial intelligence and machine learning in optical fiber sensors provides a significant increase in accuracy. Paper [7] demonstrated that neural network algorithms significantly improve anomaly classification. However, adopting such approaches to low-cost fiber optic cable monitoring systems remains an unresolved issue.

Combined methods based on φ-OTDR are also developing rapidly. Study [8] shows that a combination of wavelet decomposition and improved ResNet provides high event classification accuracy. However, the need for expensive equipment and the complexity of implementation under real-world conditions limit practical application.

Ultra-long φ-OTDR systems are finding application in pipeline monitoring. Study [9] demonstrated that the method can localize events over tens of kilometers. However, the technology's focus primarily on infrastructure facilities rather than communication lines, and its high cost, leave open questions for telecommunications.

The dual-channel φ-OTDR approach has been successfully used for traffic flow monitoring. Paper [10] demonstrates that using two fibers improves vibration detection accuracy. However, hardware complexity and implementation cost remain significant limitations.

The TFF-CNN framework offers a new approach to intrusion detection in distributed optical systems. Study [11] demonstrated that two-dimensional feature analysis using convolutional neural networks provides high accuracy in real time. However, the dependence on expensive laser sources makes the approach economically challenging.

Vibration event recognition methods based on φ-OTDR are also being improved. Study [12] demonstrates that neural network analysis of spectrograms enables rapid event classification. However, the high cost of equipment remains a key barrier to widespread adoption.

Multiphysics analysis of pipeline leaks using distributed sensors opens new horizons. Paper [13] confirms that combining acoustic, temperature, and strain data improves localization accuracy. However, this approach has not yet been adapted to the problems of protecting communication cables.

Monitoring concrete bridges with distributed optical sensors is also actively developing. Study [14] shows that integrating fibers into structures enables deformation detection. However, the complexity of calibration and high cost limit the scalability of the technology.

Studies of pipelines subject to bending and denting complete the picture. Paper [15] illustrates the modeling of deformation-fiber interactions. However, the application of this method in telecommunication networks remains an unexplored area.

Low-cost fiber-optic intrusion detection sensors are attracting attention due to their affordability. Work [16] demonstrated that a microbending sensor detects changes in light intensity. However, scaling to long lines remains an unsolved problem.

Additional optical losses due to mechanical stress have been studied in detail. Paper [17] established a link between microbending and increased power loss. However, the practical implementation of this relationship in continuous monitoring systems has not yet reached the level of a ready-made solution.

Fiber-optic sensor-based information-measuring systems for monitoring rock deformations are also of interest.

Study [18] demonstrated that this method effectively records displacements in the rock mass. However, its application in communication cable security remains unimplemented.

Fiber-optic pressure monitoring systems for support elements continue to evolve. Study [19] confirms the feasibility of detecting changes by zone. However, adaptation to telecommunication lines has not yet been achieved.

Intelligent fiber-optic systems for monitoring concrete foundation damage are showing progress. Paper [20] demonstrated that combining sensors with AI allows for classifying structural conditions. However, scaling to long cable lines remains an open problem.

Fiber anomaly diagnostics using machine learning methods completes the review. Study [21] shows that algorithms significantly improve the accuracy of defect detection. However, design of low-cost distributed monitoring systems based on these systems still requires further research.

Our review of the literature [1–21] allows us to systematize the identified local problems in the field of fiber-optic cable monitoring into the following groups:

1) works [1, 2, 4, 5, 8, 9, 11, 12, 14] emphasize that distributed sensors based on reflectometry (φ-OTDR), Brillouin/Rayleigh scattering, and interferometry require expensive equipment (high-power lasers, reflectometers), which limits their use in distributed and intra-industrial networks. Similar issues with calibration and scaling are noted in [3, 6, 7, 13, 15, 16];

2) studies [10, 17, 18, 19, 20, 21] point to the insufficient adaptation of methods to real-world conditions (external vibrations, noise, temperature fluctuations), as well as a focus on local measurements without effective continuous monitoring of extended lines. In particular, amplitude and microflexure sensors do not enable timely detection of unauthorized access without false alarms;

3) general reviews [1–4, 6, 7] and applied studies [13–16, 21] demonstrate that existing approaches are focused on infrastructure assets (bridges, pipelines, tunnels) but are not adapted to telecommunication networks with an emphasis on simplicity and low cost, leading to gaps in mass implementation.

Thus, despite advances in fiber-optic sensor technology, the identified local problems boil down to a common unresolved issue: the lack of affordable and easy-to-implement means for continuously monitoring the integrity of fiber-optic data transmission lines and promptly detecting unauthorized access. This confirms the feasibility of conducting research focused on the development and experimental validation of a principle for monitoring the technical condition of fiber-optic cables based on analyzing changes in the pixel structure of the optical spot formed by cladding radiation under mechanical stress, with the aim of creating a low-cost automatic monitoring system. The potential application of the research results includes the design of operational prototypes of intra-zone systems for monitoring the technical condition of telecommunications in populated areas and at industrial enterprises.

3. The aim and objectives of the study

The objective of our study is to design an automated system for real-time monitoring of the technical condition of fiber-optic cables. This will confirm the feasibility of developing simple, scalable, and cost-effective automated fiber-optic communication line monitoring systems that enable the timely detection of mechanical impacts and cable integrity violations without the use of complex and expensive interferometric and reflectometric technologies.

To achieve this goal, the following tasks were set:

– to define and scientifically substantiate a principle for monitoring the technical condition of fiber-optic cables based on intelligent optical-digital analysis of the pixel structure;

– to design a hardware and software system (HSS) implementing high-frequency image capture, intelligent processing of negative light spots, pixel structure analysis, and noise compensation;

– to develop a laboratory prototype of ATCMS and conduct an experimental study to evaluate its sensitivity to mechanical impacts on the fiber-optic cable;

– to study the generation of interference during HSS operation and evaluate its level.

4. Materials and methods

The object of our study is the process of monitoring the technical condition of fiber-optic cables based on the recording and analysis of changes in the pixel structure of the optical spot formed by cladding radiation under mechanical stress.

The principal hypothesis assumes that mechanical stress on a fiber-optic cable leads to changes in the pixel structure of the optical spot formed by radiation propagating along the cladding of the optical fiber, and that these changes can be reliably recorded and analyzed using a high-resolution photomatrix without resorting to interferometry, reflectometry, or fiber Bragg gratings.

Prior to the study, the following assumptions were adopted: the optical fiber is considered a homogeneous medium without local defects; mechanical stress causes microbending without damaging the fiber structure; temperature and external electromagnetic influences do not significantly affect the experimental results; and the parameters of the optical radiation source remain stable throughout the entire measurement period.

The following simplifications were accepted during the study: analysis was conducted for a single-mode G.652 optical fiber without taking into account the effects of cladding inhomogeneities; quasi-stationary mechanical stress conditions were considered; long-term degradation processes in the fiber were not considered; image processing was performed without compensating for nonlinear distortions in the optical system, allowing for a focus on assessing the fundamental performance of the proposed system.

The study proposed a principle for monitoring changes in the numerical pattern of pixels in the optical spot projected by the cladding onto the surface of a high-resolution photomatrix, followed by hardware and software data processing using artificial intelligence and machine learning algorithms. It was also proposed to exclude changes in the parameters of the optical wave propagating along the core from the analysis. To achieve this, a negative image of the optical spot was used, and the change in the numerical pattern formed during mechanical stress on the optical fiber, when some of the optical radiation escapes into the cladding, was analyzed. The originality of the idea is its new principle for processing data obtained from fiber-optic sensors of extended objects. The proposed method does not use optical interferometry, reflectometry, and their modifications, or fiber Bragg gratings. These methods and approaches are reported in detail in the scientific literature [2–4]. However, they have a number of limitations that hinder their widespread use in various industries and human practices. The basis of this method was partially discussed in paper [9], in which one can find the mathematical apparatus and a description of the principle of monitoring additional optical power losses using a high-resolution photomatrix. The hardware and software system operates with a portion of the optical radiation propagating along the fiber cladding, which leaves the core as a result of mechanical action (microbending). This method, based on the registration and analysis of cladding radiation, was previously used to design rock displacement sensors [10] and to monitor the technical condition of reinforced concrete structures [11]. In our study, it is used to build a system for monitoring the integrity of fiber-optic communication cables.

The research and experimental methods were based on well-known laws of physics in optics. Specifically, the photoelastic effect, which occurs when mechanical stress is applied to the lateral surface of an optical fiber, is utilized. This mechanical stress causes microbending, which in turn leads to a change in the refractive index, causing some of the radiation to escape the core and enter the cladding. As previously mentioned, optical fiber was studied under mechanical stress on its lateral surface, causing microbending. This study was aimed at designing sensors for monitoring rock displacement and providing timely warning of the risk of mine collapse [9].

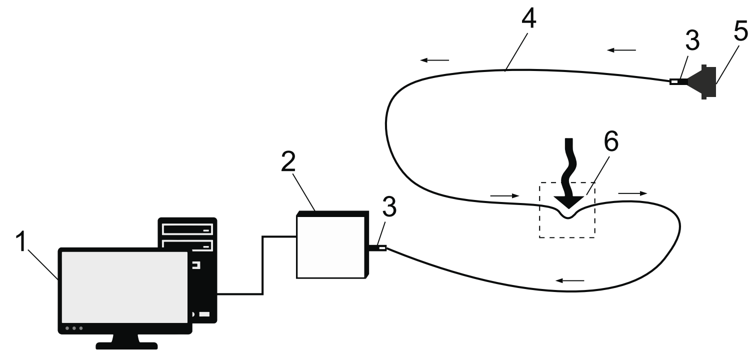

Fig. 2. Operating principle of the fiber-optic sensor: 1 — personal computer equipped with specialized software for processing and analyzing information; 2 — data processing unit with a highly sensitive photodetector (photomatrix); 3 — optical connector (detachable or non-detachable connector); 4 — single-mode optical fiber (OF); 5 — radiation source — semiconductor laser with a wavelength of 650—1550 nm; 6 — area of application of mechanical action on the optical fiber

Fig. 1 shows an image of the optical spot under increasing mechanical stress. Increasing stress leads to increased microbending of the optical fiber and, consequently, to increased additional optical loss. In this study, the pixel pattern monitoring (PPM) method was used to record and analyze changes in the optical spot.

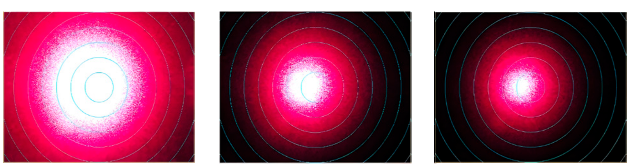

a *a* *a*

Fig. 1. Change in the optical spot on the surface of the photomatrix at different levels of mechanical load: *a* — optical spot at no load (no microbending); *b* — optical spot at medium mechanical load (formation of microbending); *c* — optical spot at maximum load (significant microbending and increase in additional losses)

The experiments were conducted using single-mode optical fiber complying with the ITU-T G.652.D standard, which is widely used in telecommunications systems. The Shijia Optical Cable GYFJH-2B1.3 IEC60332-3-16 (made in China), optical fiber type G-652 with a core diameter of 9 μm, and a cladding diameter of 125 μm was used as the object of study. The cable contained a total of 4 modules, each module containing 4 optical conductors. The optical fiber is coated with an acrylic layer on the outside to protect it from moisture; with the coating, the optical conductor thickness is 248 μm. Reserve fibers of the optical cable, which are not involved in the information transmission process, were used as fiber-optic sensors. To understand the basics of the proposed fiber optic cable design, Fig. 2 shows the general operating principle.

The laboratory prototype used one image sensor per FOD measurement channel.

During the experiments, a Full HD image sensor with a 1080p resolution, containing 1920 columns and 1080 rows, equivalent to 2,073,600 pixels, was used. To reduce the cost of the inspection system, an HD image sensor could be used; however, in this case, the image would be formed from 921,600 pixels. This could impact the sensor's resolution, as one sensor simultaneously handles at least four optical sensors. Simpler and less expensive VGA image sensors could be used, which would produce an image of 307,200 pixels. During the research, CMOS and CCD image sensors were tested. Both technologies provided the required image quality of the optical spot, but CMOS was preferred due to its lower cost and lower power consumption compared to CCD. The image sensor used must provide a light spot capture rate of at least 30 frames per second. It should be noted that CCD image sensors have demonstrated superior video image quality, but their high cost significantly increases the overall cost of the system.

During the experiments, an optical radiation source with a wavelength of 650 ± 10 nm and a power of approximately 30 mW was used. Additional optical losses were monitored during the tests. Patterns related to assessing the technical condition of optical cables and detecting unauthorized access to transmitted information were identified based on changes in optical power. When a mechanical load was applied to the fiber-optic sensor, a microbend formed in the fiber, leading to an increase in additional losses and a decrease in the light spot intensity. Experimental results showed that with a linear increase in the applied force, the light spot intensity also decreases linearly. Computer screen shots clearly illustrate the loss of optical power of a light wave propagating along an optical fiber as the load on the fiber-optic sensor increases.

The experiments demonstrated stable and reliable ATCMS operation using lasers with a wavelength of 650–850 nm. Conventional CMOS sensors from CCTV cameras with a resolution of 720p (HD) and higher, as well as webcam sensors, reliably and distortion-free record light spots even in the presence of an infrared component.

The four-channel ATCMS prototype with quasi-distributed fiber-optic sensors (including earlier versions) enables reliable monitoring of lines up to 40 km long. Using an HD 1280 × 720 sensor, the total number of sensitive elements is 921,600 pixels, while switching to Full HD 1920×1080 increases this number to 2,073,600 pixels. Increasing the resolution to Full HD significantly improves the clarity of the light spot image and the overall resolution of the monitoring system.

5. Examination of the laboratory sample of the automatic control system

5. 1. The principle of monitoring the technical condition of fiber-optic cables based on radiation analysis

The basic principles of the system's design are determined by the following parameters: the length of the fiber-optic sensor (FOS) can vary from 1 to 60 km; the operating wavelength range is 650–850 nm; and the number of FOS channels ranges from 1 to 32 per hardware and software system. Since the system uses single-mode optical fiber, it is characterized by significant losses at a wavelength of 650 nm, reaching several decibels. Therefore, for FOS cable lengths exceeding 30 km, it is recommended to use wavelengths in the 750–850 nm range. The laser power in the monitoring system is determined by the length of the fiber-optic sensor and the number of channels used. For configurations with FOS cable lengths up to 30 km, the laser source power per channel can range from 30–50 mW. When increasing the length of the fiber optic cable beyond 30 km, it is necessary to use lasers with higher output power; the power of the radiation source should be from 50 to 200 mW for each channel.

If the fiber is not subjected to mechanical stress, additional losses are absent or minimal. As the load increases, additional losses increase, and more light escapes from the fiber core and the cladding. Accordingly, the higher the load (pressure) on the fiber, the greater the level of additional optical losses. In this case, the dependence will be direct, and the nature of the approximation will be linear. This makes it possible to design a distributed or quasi-distributed fiber-optic sensor capable of monitoring overburden pressure or rock displacement. Research results related to the development of fiber-optic sensors for the mining industry have been previously published [10]. It was found that any impact on the fiber causes changes in the parameters of the optical wave propagating along the fiber core. Experiments have shown that the radiation intensity decreases as the length of the control and measuring channel of the fiber-optic sensor (FOS) increases. In this regard, for a wavelength of 650 nm, there are technological limitations on the range of application, not exceeding 60 km. Since these sensors are designed to monitor the geotechnical condition of mine workings, a sensitive area length of 3–10 km is quite sufficient.

Using the results of previous research, a hypothesis was put forward related to the design of distributed or quasi-distributed fiber-optic sensors for monitoring the technical condition of fiber-optic cables or long-distance objects (electrical cables, pipelines, gas pipelines, and others). A fiber-optic cable will be used as a sensor. Fiber integrity testing will be conducted at a wavelength of 650 nm, which does not interfere with information flows operating at wavelengths of 1310 and 1550 nm. Redundant fiber-optic cables not used for data transmission can also be used. The hypothesis implied that the entire optical spot itself would be monitored, not only its part, namely the fiber-optic cladding. As stated previously, the length of a fiber-optic control and measurement channel is limited to 60 km, so length restrictions will also be imposed on the future automatic fiber-optic cable condition monitoring system. Since future systems are planned for use in intra-zone telecommunications systems at various target sites and industrial enterprises, this wavelength is sufficient. A fiber-optic cable is used as the sensing element. Fiber integrity monitoring is performed at a wavelength of 650 nm, without affecting the 1310 and 1550 nm channels. The use of backup optical fibers not used for data transmission is permitted.

The intelligent hardware and software ATCMS system distinguishes between various types of impacts on fiber-optic cable. Specifically, the system detects unauthorized contact with the cable, including manual handling and attempts to remove the outer protective sheath to access the optical fiber. ATCMS also detects cable breaks, excessive sagging, or stretching. The red laser source operated in continuous mode. Using a 650 nm wavelength does not adversely affect data transmission over fiber-optic communication lines, as the data channels operate at wavelengths of 1310 and 1550 nm. Unit 2 contains two photo matrices, one for each measuring channel. The design of the data processing unit provides two inputs and two outputs and enables operation in dual-channel mode, which allows for redundant operation of the fiber-optic sensor and reduces the likelihood of false alarms. The data processing unit contains two independent control and measurement optical channels.

Fig. 3 shows a diagram illustrating the operating principle of the method for monitoring changes in the pixel digital image. Photomatrix 5 has its own graphics processor for pre-processing the video image of the optical spot. Photomatrix 5 converts optical signals into electrical signals, which are digitized and sent to the hardware and software system for further processing.

The proposed monitoring principle, based on intelligent optical-digital analysis of the pixel structure of the optical spot of cladding radiation, enables the recording of mechanical impacts on fiber optic cables without the use of expensive interferometric and reflectometric methods. A distinctive feature of this approach is the transition from core analysis to cladding analysis, which significantly reduces system cost, facilitates ease of implementation, and provides high immunity to external interference.

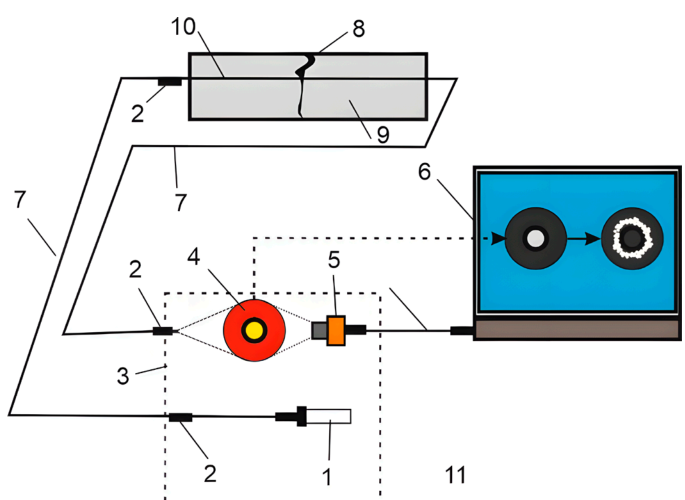

Fig. 3. Explaining the method for monitoring changes in the numerical pattern of pixels: 1 – radiation source; 2 – fiber-optic connector for optical connection of conductors. 3 – preliminary data processing unit; 4 – optical spot formed on the surface of the photodetector; 5 – photomatrix with a graphic processor; 6 – computer with specialized software; 7 – fiber-optic conductors; 8 – cable break point; 9 – section of fiber-optic cable; 10 – optical sensor located inside the fiber-optic cable

5. 2. Design of the hardware and software system

The hardware and software system continuously monitors the change in the numerical pattern of pixels as they transition from black to white.

Fig. 4 shows the internal contents of the pre-processing unit. During the development of the laboratory prototype of the automated system for monitoring the technical condition of fiber-optic cables, several modifications of the optical modules were manufactured. Each module includes a photomatrix with a graphics microprocessor, an optical adapter, a light guide, an optical connector, and an optical waveguide. The waveguide cross-section can be either round or square.

Optical adapters and SC-type connectors with a 2.5 mm diameter ferrule were used to connect the fiber optic cables. Optical power loss at each connector did not exceed 0.3 dB. To ensure reliable monitoring of the cables' technical condition using the ATCMS system and reliable detection of unauthorized access attempts, preliminary equipment configuration was required. The structure of the optical module is shown separately in Fig. 5, which demonstrates its basic components.

The ATCMS system processed data received from the fiber-optic sensor and, when the fiber optic cable was impacted, generated a warning signal; a similar response was observed during a simulated cable fault. The ATCMS software was developed using compiled programming languages with static typing. A version of the Python programming language, as well as components of the OpenCV (Open Source Computer Vision Library), were used in the system development. The optical control and measurement channels were configured in various configurations: in some cases, completely identically, while in others, they had minor differences in parameters. Fig. 6 illustrates the ATCMS interface operating under a dual-channel mode with two connected fiber-optic sensors. The module contains modules for configuring and controlling the ATCMS operating modes. During the configuration process, the photo matrices are configured and calibrated. It is possible to run the system under debug mode, which allows one to evaluate the ATCMS sensitivity.

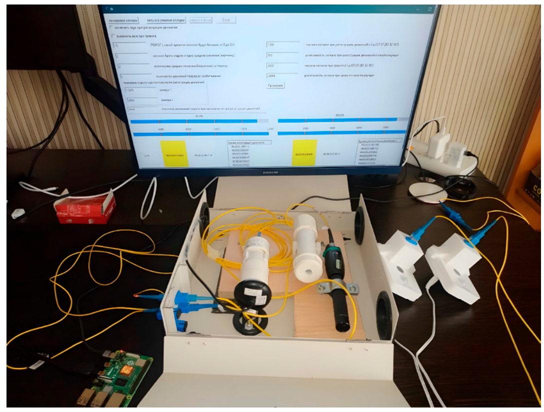

Fig. 4. Internal contents of the data preprocessing module

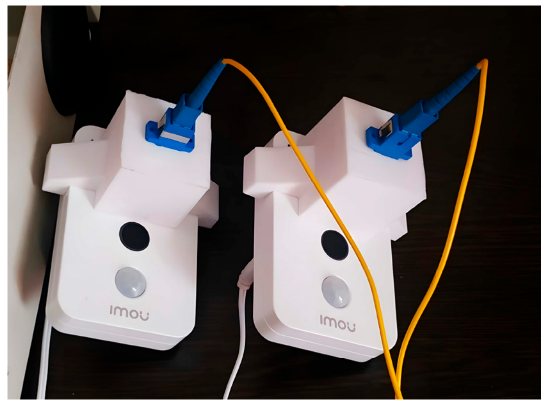

Fig. 5. Optical module with square waveguide geometry: 1 — photomatrix equipped with a graphic microprocessor; 2 — optical adapter; 3 — light guide; 4 — optical connector; 5 — square optical waveguide

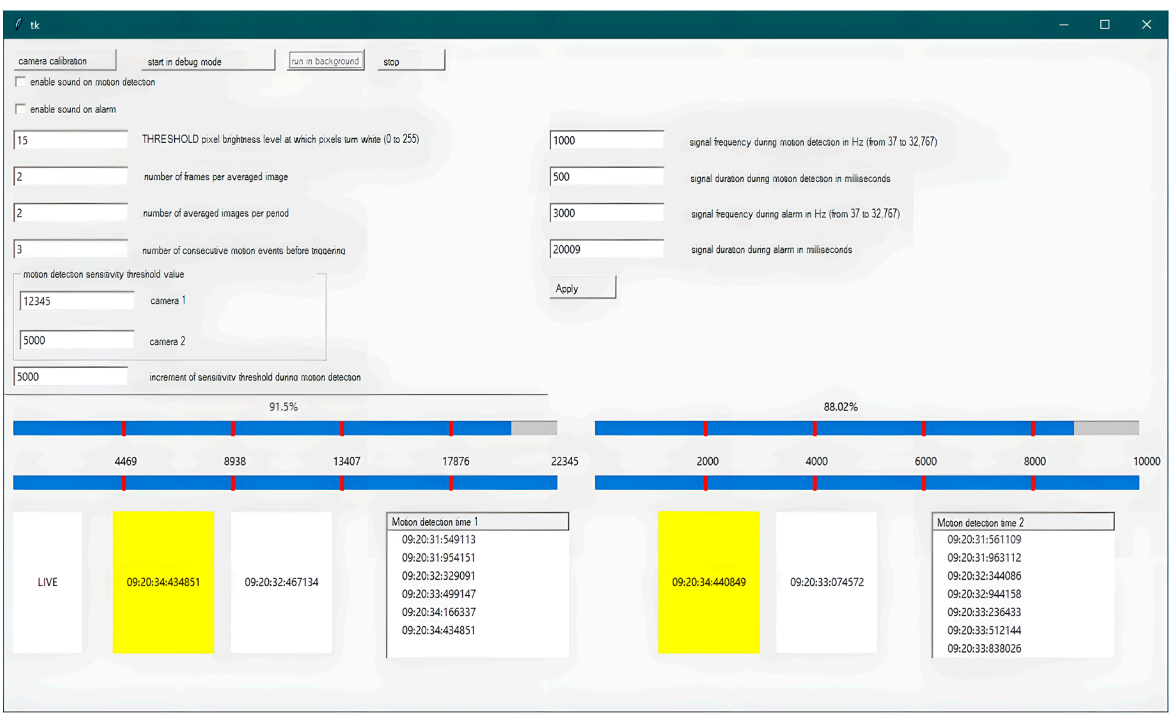

Fig. 6. Interface of the automatic technical condition monitoring system

The ATCMS has several operating modes. During normal operation, the yellow and red indicators are off. If the fiber optic cable is subjected to mechanical or vibroacoustic impact, a yellow warning indicator lights up, alerting you to a changing situation. If the impact is weaker than the response threshold or has not exceeded the repetition limit, the yellow indicator goes out after 5 seconds. If the impacts are repeated multiple times and their value exceeds the response threshold, the red indicator lights up. When the red indicator lights up, an alarm is triggered, and the operator receives a message on their mobile device (smartphone). Each channel contains two measurement scales: the lower scale shows the value of the white pixels, corresponding to the impact strength. The upper scale shows the percentage of the response threshold reached, which is related to the strength and number of impacts applied to the fiber optic cable within a set time interval (Fig. 7). When started in background mode, the ATCMS enters the operating mode for continuous monitoring of the technical condition of the fiber optic cable.

Fig. 8 shows the module for setting the ATCMS response threshold.

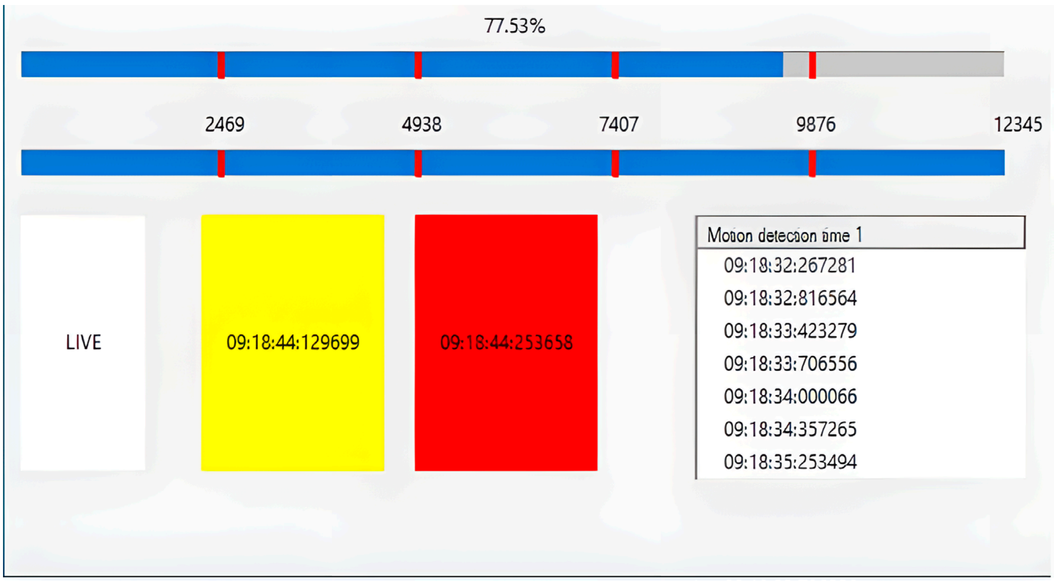

Fig. 7. Indicators and scales of the automatic technical condition monitoring system

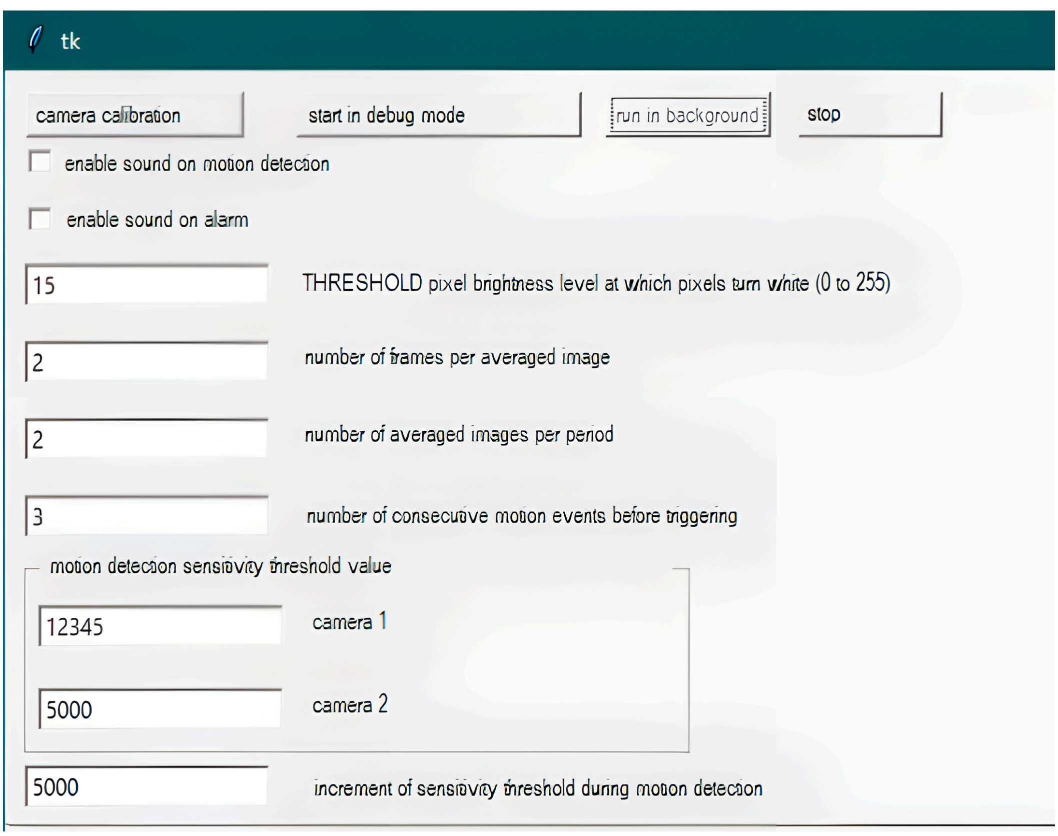

Fig. 8. Module of settings for the response threshold of the automatic technical condition monitoring system

The ATCMS hardware and software system converts changes in the light spot parameters, registering the level of additional optical losses; the system generates a corresponding pixel map. Fig. 9 shows how the structure of the pixel distribution of the light spot (LS) changes under the influence of external forces applied to the optical fiber (OF); Fig. 9 shows a sequence of six positions, each reflecting the degree of pixel change as the external force acting on the OF increases. As the force acting on the OF increases, microbending increases, causing an increase in additional losses and a change in the light spot intensity. This is visually manifested as a transition of pixels from black to white. In Fig. 9, positions 1 and 2 indicate a minor impact, with the number of white pixels being minimal, indicating a weak impact on the OF. Positions 3 and 4 demonstrate a more significant impact, with the intensity of changes in the LS increasing, reflected by an increase in the number of white pixels in the central part of the spot. Position 5 demonstrates the most intense exposure, where the majority of pixels switch to a white state, indicating a significant change in the light wave characteristics and an increase in additional optical losses. Thus, increasing external exposure to the fiber optic sensor leads to a proportional increase in the number of white pixels, reflecting an increase in the level of additional losses and a change in the phase and amplitude characteristics of the optical wave.

Fig. 10 shows a window for adjusting the photo sensor.

For monitoring fiber-optic communication lines up to 60 km long, a visible-range laser source with a power of less than 200 mW is sufficient. A possible reduction in the brightness of the light spot at the far end of the line is fully compensated for by adjusting the sensitivity of the photomatrix and software signal processing algorithms.

Switching to the invisible infrared range (900–1550 nm) would require the use of specialized IR-sensitive photo matrixes and significantly more expensive infrared lasers, which would dramatically increase the cost of the entire system.

Fig. 11 shows the results of computer simulation of the optical spot image. Computer interpretation of the optical spot is more clearly understood for understanding the method, as it is sharper and closer to ideal. The left side of Fig. 3 shows an image of the optical spot formed on the surface of the photomatrix. The photomatrix is installed at the end of the optical fiber (Fig. 11, *a*). The image is shown as a positive; since radiation with a wavelength of 650 nm is used, shades of red are visible. When using a single optical fiber, the spot structure is characterized by maximum brightness in the central area.

The core forms a fairly bright, almost white spot and illuminates the matrix. Optical radiation, which has a Gaussian normal distribution, propagates continuously through one optical fiber. The first region is uninformative and essentially noise. Further on, the transition boundary from white (white-yellow) to pink and bright red is visible; this is the second region. Further on, the ring of the third red region is clearly visible. The ATCMS hardware and software system operates on the second and third regions, which change their intensity when the optical fiber is mechanically stimulated. The ATCMS hardware and software system converts the positive image into a negative (Fig. 11, *b*). In the negative, the first region is excluded from analysis and appears black. Regions 2 and 3 contain white pixels; the greater the microbending of the optical fiber under pressure or mechanical stress, the whiter pixels will be in regions 2 and 3.

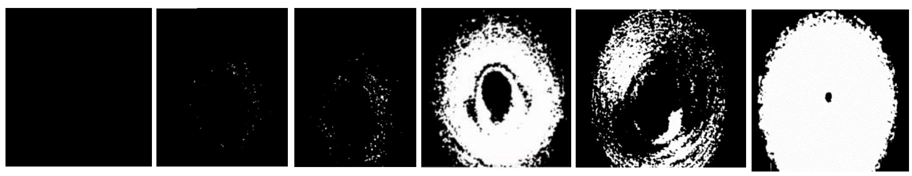

Fig. 9. Image of a computer screen

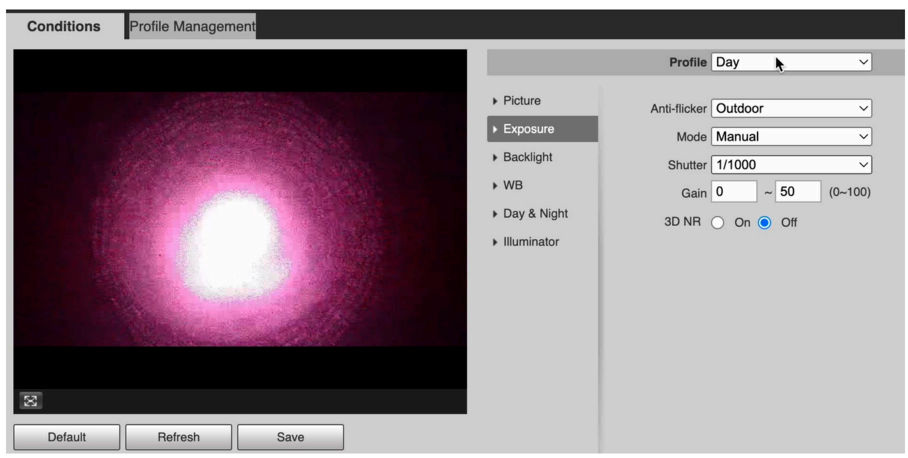

Fig. 10. Window for adjusting the photo sensor

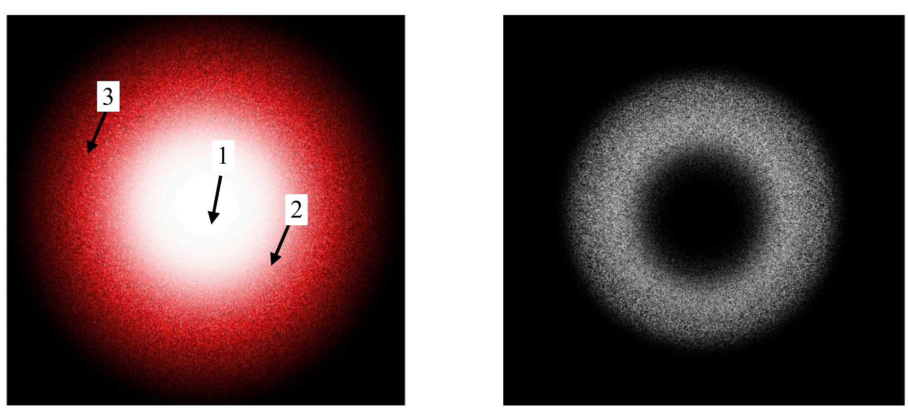

a *b*

Fig. 11. Image of pixels on the surface of a photomatrix: *a* — positive image of a light spot formed on the surface of a photomatrix when radiation passes through an optical fiber; *b* — negative of a light spot used to highlight informative areas in optical-digital analysis

5. 3. Results of the design and experimental studies of a prototype automatic system for monitoring technical condition

A laboratory prototype (Fig. 12) was specially designed for the experiments, allowing for testing of the ATCMS hardware and software. This setup was later used as the basis for a future experimental prototype, which is planned for testing under critical conditions in real production. The setup has a simple design and includes the following main components: a computer 1, a pre-processing unit 2, optical connectors 3 for connecting a fiber-optic sensor 4, and a spool 5 on which the fiber-optic cable is wound.

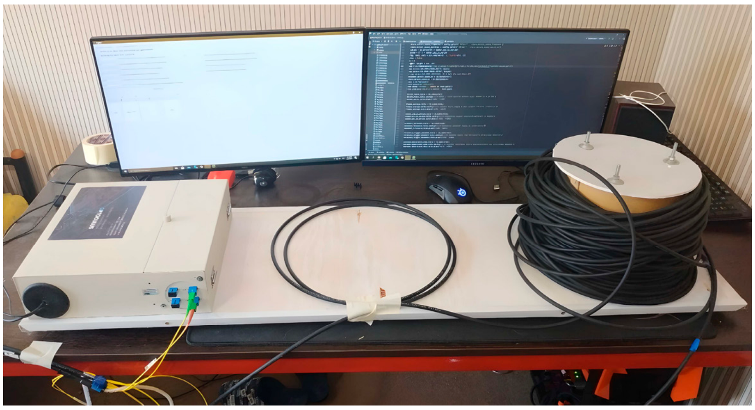

Fig. 12. General view of a laboratory sample of an automatic system for monitoring the technical condition of fiber-optic cables

The bench consists of a structure with a 16 mm thick plywood base, onto which a reel with a fiber optic cable approximately 200 meters long is attached. The Shijia Optical Cable GYFJH-2B1.3 IEC60332-3-16 (made in China) was used as the test object. Mechanical action was applied to loop 4, located on the base of the bench. The loop was specially formed from several turns of fiber optic cable and was used as a sensing element responding to external influences. The impact object was a hammer with a head weighing 500 g and a soft rubber striker. The technique involved a free fall from a height of 2–7 cm (without swinging), followed by controlled tapping of random nature. This method was chosen to simulate unauthorized access, in which the impact is random. The hammer exerted an impact without applying external force to eliminate the increase in impact energy. The drop height was recorded using a measuring ruler, with an error of within 5 mm. After the impact, the hammer returned to its original position, and its height was again recorded. The room temperature and humidity remained constant throughout the experiment, which had no effect on the linear dimensions of the cable. When the ATCMS was launched, the program window displayed a zero value of white pixels, indicating the level of additional losses generated in the fiber optic cable due to microbending. Microbending occurs through mechanical action directly on the fiber optic cable jacket. Microbending can be caused by various methods, such as bending or by striking the side of the fiber optic cable with a heavy object. The latter method was chosen for the experiment. The measurement results were slightly affected by generated interference, which was recorded by ATCMS. The maximum value of generated white pixels did not exceed 100 units. Under mechanical stress, the values of the formed white pixels range from units to tens of thousands, thus enabling the system to evaluate and distinguish laser-generated interference from the useful signal under mechanical stress.

The setup utilized a 650 nm semiconductor laser mounted on one end of the optical fiber and a photodetector on the opposite end as a radiation source. The collected data is transmitted to a processing unit. Unlike traditional fiber-optic monitoring systems, this experiment utilized a 650 nm laser (in the visible red light range), which is not typical for single-mode fiber complying with the G.652 standard. The refractive indices satisfy the relation $n_1 < n_2$, where $n_2 = 1.4625$ corresponds to the core, and $n_1 = 1.4570$ corresponds to the cladding. Due to the lower cladding density compared to the core, virtually total internal reflection of the beam is achieved within the fiber core, ensuring its efficient propagation. In reality, optical signal attenuation ranges from 30 to 100 km, depending on the fiber type. Optical wave attenuation decreases with increasing wavelength and is achieved in the third transparency window at 1550 nm. The proposed method utilizes a 650 nm laser and a high-resolution image sensor, which is justified by the lower cost and simplicity of the monitoring system, increasing the likelihood of implementation. Unlike existing fiber-optic sensors, which rely on a photodiode to detect changes in optical radiation, the proposed method utilizes a high-resolution image sensor. The image sensor records changes in the optical pattern of a spot incident on its surface, but only the radiation propagating along its cladding. The intelligent optical-digital analysis excludes the optical pattern formed by the fiber core. Existing fiber-optic sensors, such as amplitude sensors, rely on changes in the amplitude of the optical wave propagating along the core. The proposed method evaluates the additional losses generated in the cladding and reaching the image sensor. The amplitude of the optical signal generated in the core is not considered.

Fig. 13 shows a schematic diagram of a laboratory-scale ATCMS prototype. When mechanical stress is applied to the optical fiber, a microbend is formed at point 7, causing some of the optical radiation to escape the core and propagate within the fiber cladding. Additional losses, directly related to the stress intensity and the optical radiation intensity level, correspondingly alter the optical spot pattern, or pixel pattern. The greater the stress force causing the microbend, the higher the additional losses and the lower the intensity. These changes are linear. Solid arrows indicate the propagation of optical radiation from the laser toward the photodetector. The laboratory setup makes it possible to simulate unauthorized access or damage to the cladding, as well as various mechanical stresses. A diagram of the setup is shown in Fig. 13.

When a fiber-optic cable is subjected to mechanical stress, deformation is transmitted to the optical conductors. Consequently, when a mechanical stress is applied to the side of the cable, the stress is transmitted to the optical waves beneath its cladding. Changes in the optical radiation parameters are recorded by a photodetector, and a hardware and software system processes the data and produces numerical results for the pixel pattern changes.

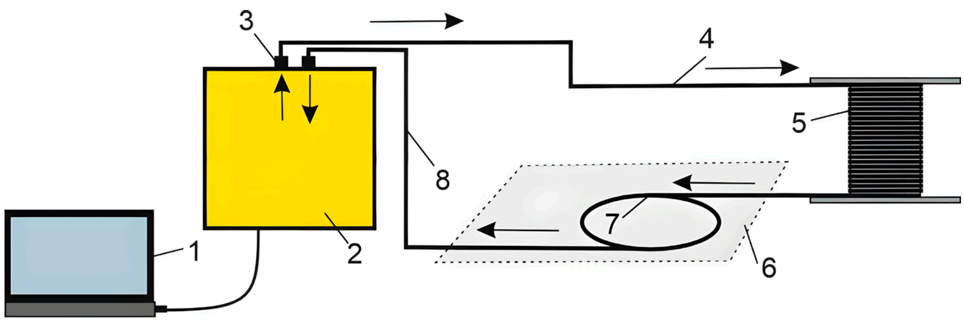

Fig. 13. Schematic diagram of a laboratory prototype of an automatic technical condition monitoring system: 1 — personal computer with specialized software; 2 — pulse generation and data pre-processing unit; 3 — connectors for connecting a fiber-optic cable; 4 — forward fiber-optic cable; 5 — spool with optical fiber; 6 — base for fixing the spool; 7 — fiber-optic loop; 8 — reverse fiber-optic cable

The photomatrix converts the optical signal into an electrical signal, which is then fed to a data processing and visualization device. When a fiber-optic cable is subjected to mechanical stress, the resulting deformation is transmitted to the optical fiber. As noted previously, such stresses lead to the formation of microbends, accompanied by changes in the light wave parameters, including the phase and intensity of its propagation, which are recorded by the photodetector. The proposed optical-digital analysis of the optical radiation parameters generated on the surface of the photomatrix is based on an original approach that significantly differs from existing methods of optical interferometry, reflectometry, and the use of fiber Bragg gratings. Using an intelligent hardware and software system, changes in the pixel structure of an optical spot are analyzed, which fundamentally distinguishes the proposed approach from conventional methods that only record changes in the scattering or amplitude of optical radiation.

Computer 1 is equipped with specially developed software that monitors changes in optical parameters in real time. The computer is connected to the pre-processing unit via a USB cable, forming a single hardware and software system. The fiber-optic sensor is connected using optical connectors, ensuring reliable and accurate connections. The fiber-optic sensor is a section of fiber-optic cable, part of which is wound onto spool 5. The arrows indicate the direction of laser radiation propagation along the fiber-optic cable from the source to the photodetector through loop 7, which serves as the sensing element. Laser radiation passes through forward cable 4, then through coil 5, and enters loop 7. Loop 7, subjected to mechanical stress, is positioned on base 6. The optical radiation then exits loop 7 and returns via return cable 8 to pre-processing and pulse generation unit 2. Thus, the optical wave completes the propagation cycle from the radiation source to the photodetector. All changes in the optical wave parameters were recorded by the photomatrix, and after processing, a numerical result of the pixel pattern changes was output. Mechanical stress on loop 7 resulted in changes in the optical wave parameters, specifically a decrease in intensity and an increase in additional losses.

Based on the processing of experimental data on mechanical impacts on the fiber optic cable and the identification of the relevant factors, a diagram was constructed (Fig. 14). During the tests, 100 different external mechanical impacts were applied to the fiber optic cable loop, with the ATCMS system successfully recording events in 85 cases, responding to impacts of varying intensity. All impacts were random in both the level of applied force and the number of pulses, including even light touches to the fiber optic cable sheath, which did not physically deform it at a given point in time.

The results of testing the ATCMS prototype confirmed its functionality and demonstrated the high reliability of the quasi-distributed fiber optic sensor when impacting the fiber optic cable. During the experiments, the probability of correct system response to impact on the fiber optic cable was 0.85, with the error rate not exceeding 15%. In the future, it is planned to increase the response probability to 0.9, while simultaneously reducing the probability of false alarms to no more than 0.1. An analysis of the probabilistic characteristics of the quasi-distributed fiber-optic sensor is depicted in Fig. 14.

When the program is correctly configured and running under a normal (operating) mode, both interface windows – the window displaying the light spot and the window displaying real-time graphs – remain completely black. All indicators (the number of white pixels, their total brightness, and the average intensity by sector) consistently show values close to zero (typically 0–5 units on a 0–255 scale). This behavior is normal and directly confirms the system is functioning properly.

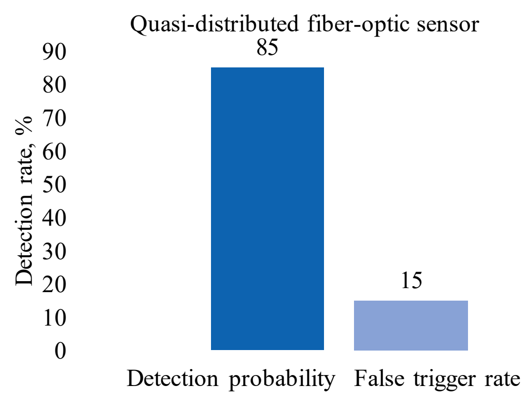

Fig. 14. Analysis of probabilistic characteristics of a quasi-distributed fiber-optic sensor

The absence of a visible light spot is explained by the fact that, after stabilization, residual pulsations in the radiation source are reduced to a minimum (Fig. 15, 16). The fiber optic cable experiences no mechanical stress, such as bending, compression, or vibration. Optical radiation propagates along the path with virtually no additional loss, and a uniformly dark field with minimal intrinsic noise is formed on the image sensor. As a result, the brightness of the light spot is either zero or extremely low, which is visually perceived as a completely black frame.

The visualization of the light spot image, heat maps, histograms, and dynamic plots is activated only under a special debug mode. Under a normal operating mode, these elements are intentionally hidden to avoid unnecessary load on the processor and graphics card. Meanwhile, the automated software suite continues to operate in the background: capturing frames at a rate of 100–200 per second, performing intelligent processing of each frame, calculating the spot intensity and sector-specific indicators, comparing them with reference and adaptive thresholds, and instantly responding to any anomalies indicating mechanical impact, microcracks, or destabilization of the radiation source.

Therefore, completely black windows and virtually zero graph values under an operating mode are not an error but a reliable indication that the monitored section of fiber optic cable is in perfect technical condition, and the monitoring system is functioning properly and is ready to detect and record even the slightest external impact at any time. During the initial launch, there was no interference generated by the semiconductor laser, which later appeared due to its heating.

The designed fiber-optic cable condition monitoring system, based on the analysis of additional optical losses, has demonstrated high efficiency in detecting mechanical impacts. Monitoring is achieved by recording changes in the intensity of visible radiation incident on the surface of the photodetector's sensitive element, ensuring accurate and prompt detection of external interference. Fig. 16–19 show plots of recording mechanical impacts of varying intensity on the fiber-optic cable under conditions of simulated unauthorized access. The key conclusion is that the ATCMS system reliably responds to external impacts, recording them based on additional losses occurring in the line. Moreover, the optical monitoring channel with reduced sensitivity demonstrates immunity to external interference and parasitic influences. Fig. 16 shows a screenshot of the fiber-optic cable subjected to the weakest repeatedly verified mechanical impact: dropping a hammer with a head weighing 500 g and a soft rubber striker from a height of 3 cm (without swinging). Fig. 16 shows how the pixel pattern has changed and their maximum value has reached 2193 units.

Fig. 17, 18 show two strong mechanical impacts on the loop from a height of 4 and 6 cm, respectively, which were successfully recorded by the ATCMS system.

In the first case, changes in the pixel pattern are visible, with their maximum values reaching 52,156 and 49,751 units (Fig. 17). In the second case, two effects were recorded, which were stronger than in the first case. The maximum values of white pixels reached 52,156 and 49,751 units.

Fig. 19 shows the increasing white spot on the computer screen and the number of white pixels. In these cases, the optical fiber was subjected to mechanical impact by dropping a hammer with a 500-g head and a soft rubber striker from a height of 7 cm (without swinging), inducing maximum bending of the optical fiber.

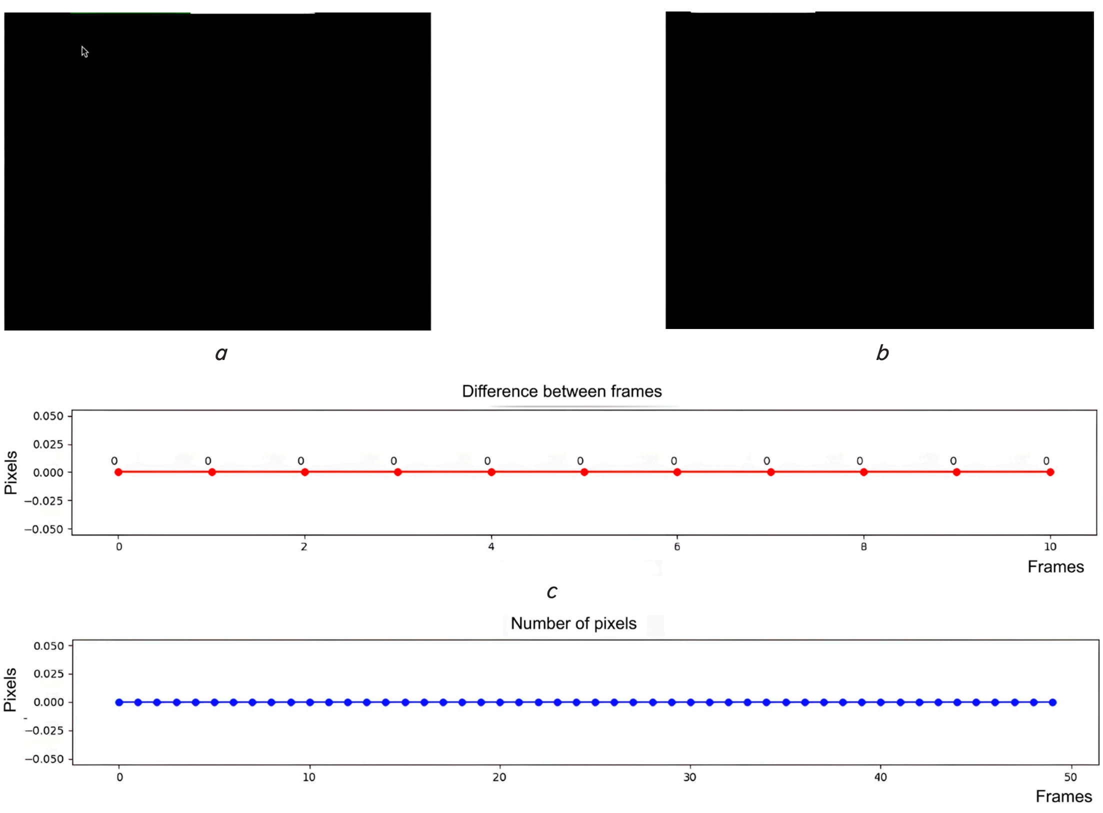

Fig. 15. Parameters of the monitoring system operation under a normal mode: *a* – image of the difference between the reference and current frame in the absence of external influences; *b* – binarized image with a minimum number of white pixels not exceeding the sensitivity threshold; *c* – plot of the instantaneous rate of change in the number of white pixels over time; *d* – plot of the total number of white pixels in successive frames

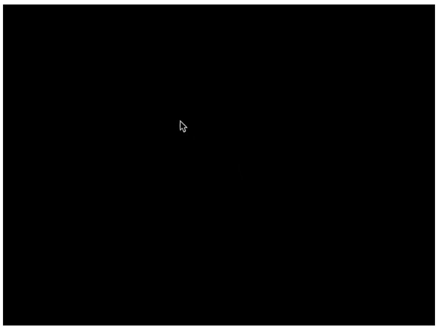

a

b

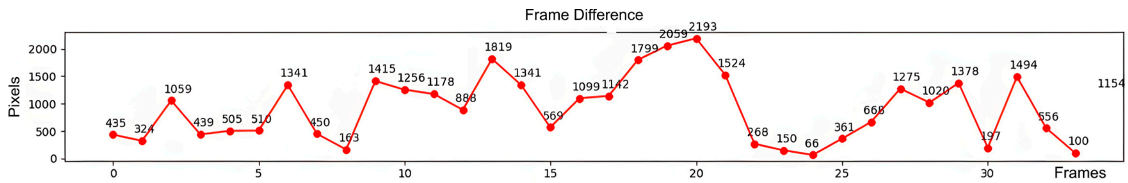

c

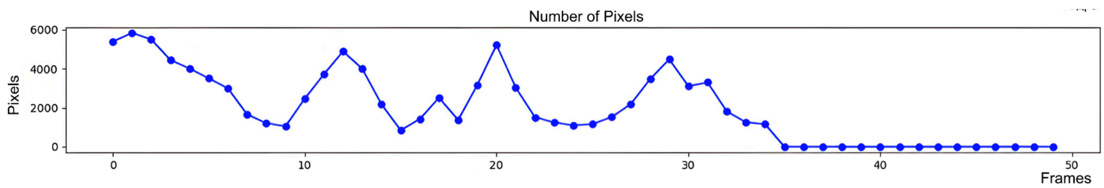

d

Fig. 16. Plots that record mechanical impacts on a fiber-optic cable during the simulation of unauthorized access: *a* — change in the spatial structure of the light spot with minimal mechanical impact; *b* — binarized image of activated pixels after exceeding the threshold value; *c* — plot of the rate of change in the number of white pixels with repeated impacts; *d* — plot of the total number of white pixels over time

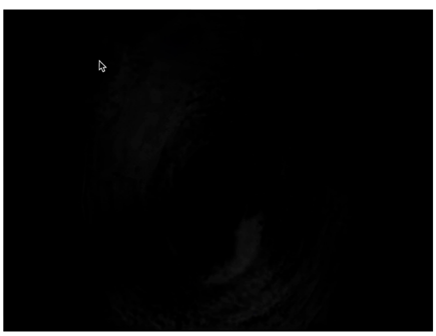

a

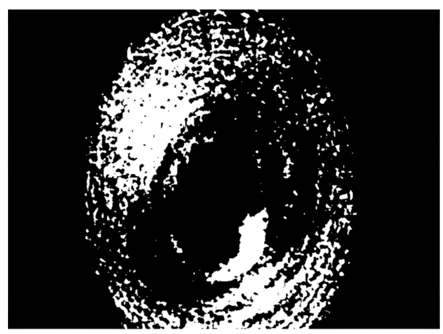

b

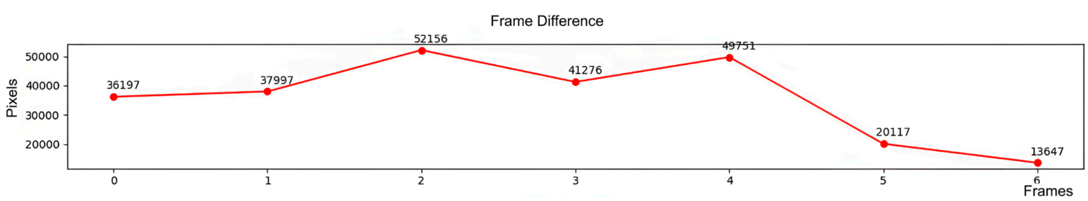

c

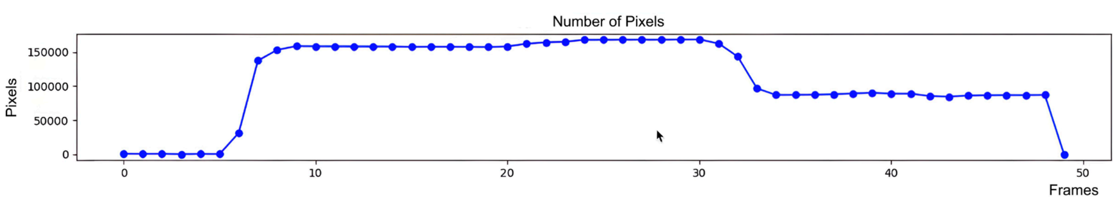

d

Fig. 17. Plots that record impacts on a fiber-optic cable during the simulation of an attempt at unauthorized access: *a* — deformation of the light spot during a strong mechanical impact on the fiber-optic cable; *b* — binarized image with a high density of white pixels; *c* — plot of the intensive growth rate of change in the number of white pixels; *d* — plot of the total number of white pixels during the impact

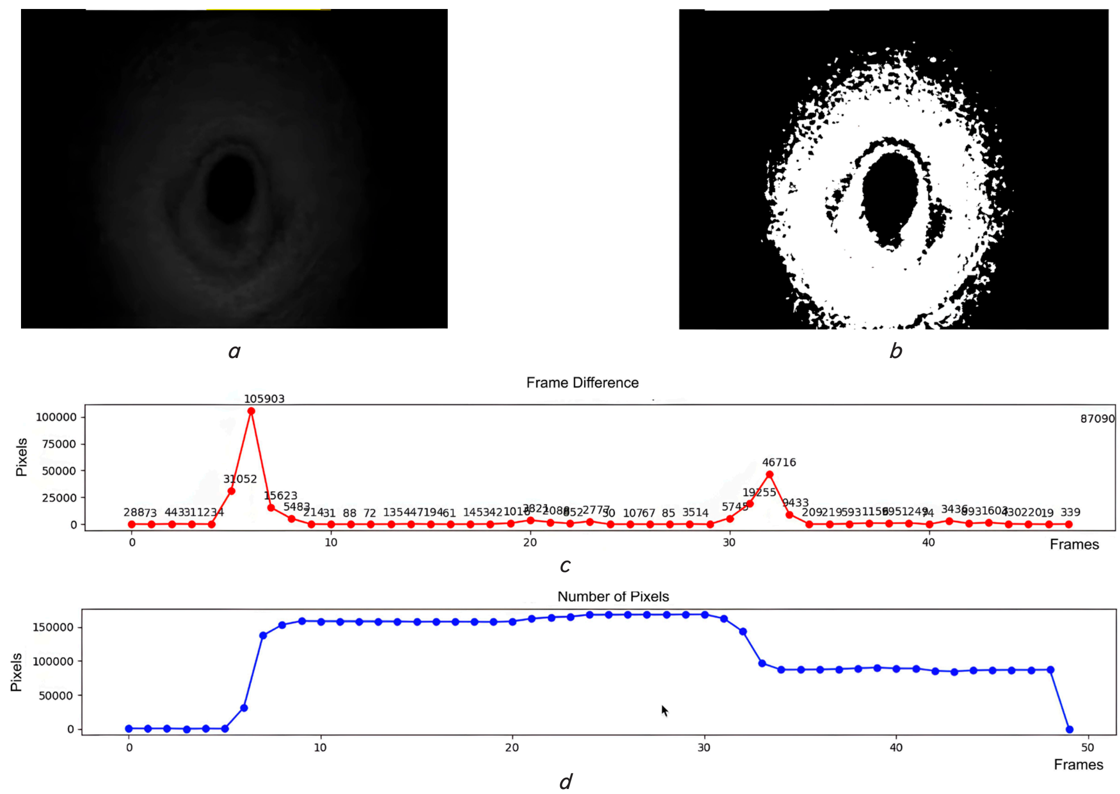

Fig. 18. Plots that record impacts on a fiber-optic cable during an attempt to achieve unauthorized access: *a* – change in the image of a light spot with repeated mechanical impacts; *b* – binarized image of pixels registered by the system; *c* – plot of the rate of change in the number of white pixels with successive impacts; *d* – plot of the total number of white pixels over time

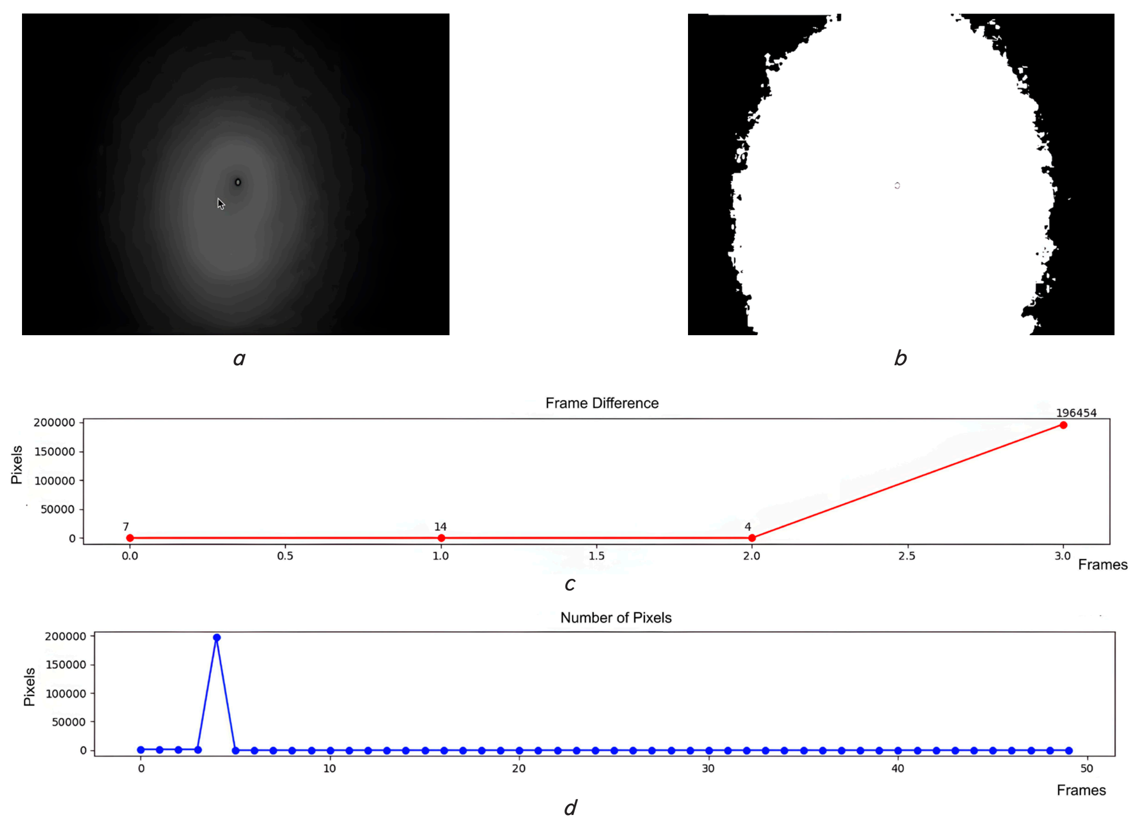

Fig. 19. Plots that record impacts on a fiber-optic cable during an attempt to achieve unauthorized access: *a* – growth and deformation of the light spot at maximum bending of the fiber-optic cable; *b* – binarized image with the maximum number of activated pixels; *c* – plot of a sharp increase in the rate of change of the number of white pixels; *d* – plot of the maximum total number of white pixels registered by the system

Changes in the pixel pattern are visible, and their maximum value reached 196,554 units (Fig. 19). In the second case, stronger changes were recorded than in the first.

5. 4. Studying interference generation during operation of a hardware and software system

The experiment was conducted on a laboratory prototype of a fiber-optic cable (single-mode G.652.D fiber). The light source was a laser diode, and the optical spot was recorded by a CMOS image sensor (1920 × 1200 pixels, 5.86 μm pixel size, 12 bits, 30 fps).

The mechanical load was generated by using a hammer with a 500 g head and a soft rubber striker from a height of up to 7 cm (without swinging). The load varied from 0 to 5 N, with a total of 100 measurements. Conditions: temperature 23 ± 2°C, humidity 45 ± 5%, illumination < 10 lux, matrix gain 0 dB, exposure 1/1000 s. The following parameters were recorded: average brightness I_{ave} (0–4095 units), the number of pixels above the threshold $I_{threshold}$ = 500 (N_{pix}). It should be noted that the distribution of the points forming the light spot is characterized by pronounced non-uniformity, especially in the region of the boundary between the core and the cladding of the optical fiber. The HSSTCM system enables reliable discrimination between real mechanical impacts on the fiber-optic sensor and interference caused by external factors, such as fluctuations in ambient temperature or gusts of wind affecting the fiber optic cable. Fig. 20 shows the results of computer simulation of the dynamics of changes in interference parameters. Interference arises due to a minor effect of temperature, but the greatest interference can be caused by external vibroacoustic waves not related to direct impact on the fiber optic cable during ND. The screen displays two clouds of points, which can be interpreted as the result of external noise or laser incoherence. These factors manifest themselves in the appearance of random points, which differ significantly in number from those generated by external force applied to the fiber optic cable. The plot shown at the bottom of Fig. 20 illustrates the change in the number of points recorded over time. It can be seen that the number of pixels fluctuates between 50 and 75 depending on time, which may be due to various factors. Despite the presence of interference, its number is significantly lower than the number of pixels recorded during an attempt at unauthorized access to the protected fiber optic cable. Experimental data have shown that interference caused by incoherence and noise in the radiation source can occur in the measurement channel; however, their impact on the final result is insignificant and incomparable to the effects observed when the fiber optic cable is damaged.

The designed HSSTCM system is characterized by high noise immunity in the measurement channels. It analyzes changes in the pixel structure of the light spot and generates an alarm upon detecting signs of unauthorized access (UA). The system is also capable of assessing the number of impacts, their strength, frequency, and repeatability. If the set impact thresholds are exceeded, the system automatically generates an alarm. External mechanical impact on the fiber optic cable causes a change in the intensity of the light spot, resulting in a transformation of its pixel structure: the greater the impact strength, the more pixels change their state from black to white. During experiments, isolated instances of impact exceeding the set threshold levels were recorded, resulting in the activation of the alarm system designed to protect against unauthorized access. The HSSTCM also features adjustable sensitivity, a significant advantage in the presence of external interference. Since the interference has different frequency characteristics and intensity change rates than UA, the system does not perceive it as a threat. The technique used makes it possible to track changes in the derivative of the light spot intensity, as well as the dynamics of additional optical loss growth over a specified time interval. The system is capable of tracking not only changes in the light spot intensity but also its geometric shape, performing a numerical analysis of the degree of impact on the optical fiber during microbending in real time.

During the experiments, it was established that one of the main problems is noise generated by the light source itself. Fig. 21 shows a screenshot of the recorded interference caused by source noise; the total number of white pixels did not exceed 100.

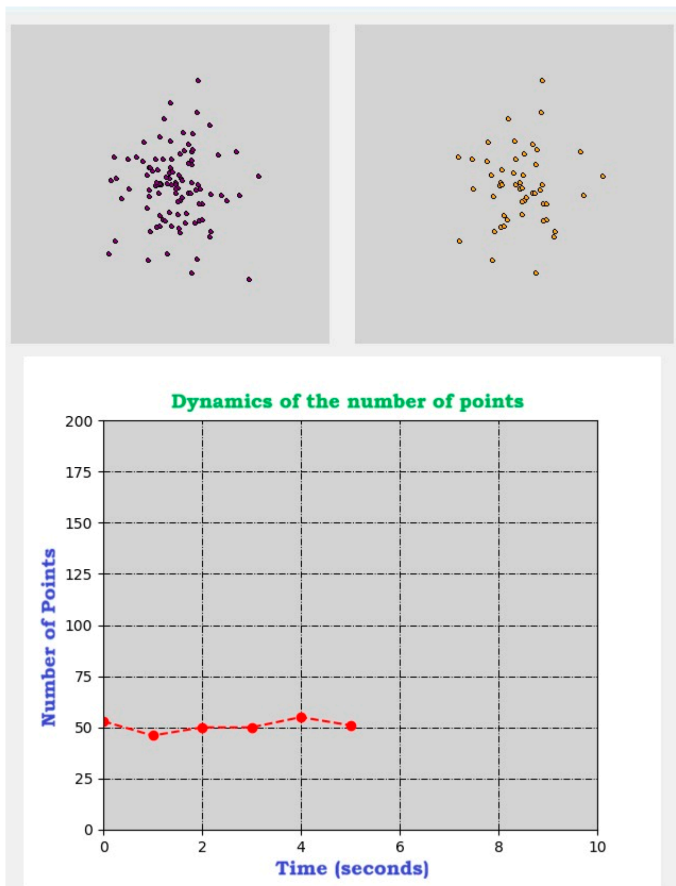

Fig. 20. Noise interference from laser radiation in the hardware and software system

This noise interference is detected by the photomatrix and can lead to false alarms. To improve the system's accuracy, it is necessary to reduce the laser beam pulsation level.

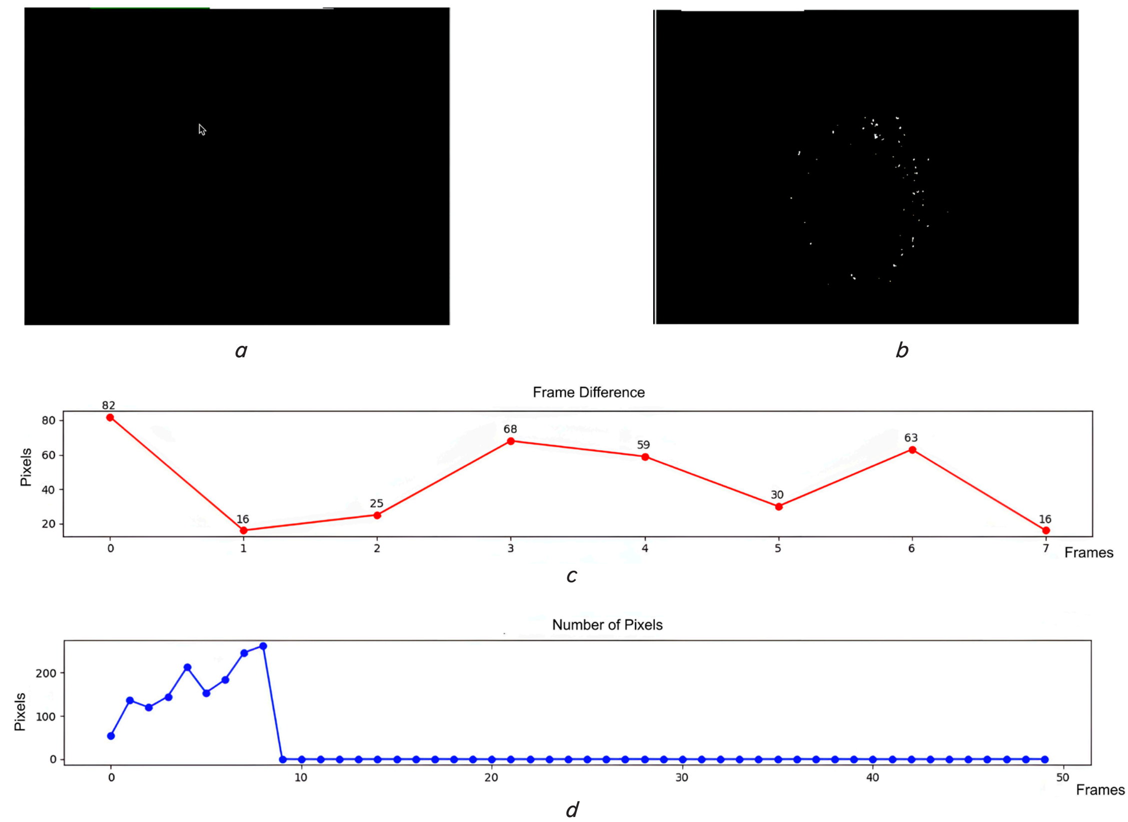

Fig. 21. Plots that record impacts on a fiber-optic cable during an attempt to achieve unauthorized access: *a* – change in the structure of the light spot with weak mechanical impact on the fiber-optic cable; *b* – binarized image of pixels registered after threshold processing; *c* – plot of the instantaneous rate of change in the number of white pixels; *d* – plot of the total number of white pixels during the impact

6. Discussion of results based on the study of a laboratory prototype of an automatic system for monitoring the technical condition of fiber-optic cables

The proposed principle for monitoring the condition of fiber-optic cables is based on intelligent optical-digital analysis of changes in the pixel structure of the optical spot formed by cladding radiation when the fiber undergoes microbending. Unlike widely used interferometric, reflectometric (φ-OTDR), and Bragg methods [2–9], this principle does not require expensive equipment or complex calibration. Recording is performed exclusively based on the radiation emitted into the fiber cladding, which is achieved by converting a positive image to a negative and then processing it using artificial intelligence and machine learning algorithms (Fig. 3). A distinctive feature of this principle is the transition from analyzing the fundamental wave in the core to analyzing the secondary (cladding) radiation. This significantly simplified the system's design, reduced its cost, and ensured high immunity to external interference (temperature fluctuations, vibrations, and electromagnetic interference). A linear relationship between the magnitude of the mechanical load and the change in the numerical pixel pattern was experimentally confirmed, demonstrating the fundamental viability and effectiveness of the proposed approach for continuous integrity monitoring of fiber-optic communication lines.

Microbending simulation results (Fig. 11) and cladding radiation analysis (Fig. 5) confirm that mechanical stress causes a noticeable increase in intensity and a change in the shape of the spot on the image sensor, which underlies the pixel pattern change monitoring (PPCM) method. This enables the recording of stress without the use of expensive equipment, ensuring high immunity to temperature and electromagnetic interference.

The designed laboratory prototype (Fig. 12) and module diagram (Fig. 13) demonstrate the simplicity of the structure: using a standard G.652.D single-mode fiber, a low-power laser source ($\lambda = 1310$ nm, $P_0 = 1.0$ mW), and an inexpensive Basler acA1920-155um CMOS image sensor. The system interfaces (Fig. 6–10) demonstrate stable real-time operation, including frame capture at 30 fps and automatic negative image processing. Our results confirm the feasibility of implementing the system using readily available components without loss of functionality.

Experimental sensitivity studies of a laboratory ATCMS prototype demonstrated a linear relationship between the magnitude of the applied load and the change in the number of activated pixels. Fig. 16–19 show typical changes in the pixel structure under impacts of varying intensities (from 5 to 50 N). In 100 tests (impacts with a 500 g hammer from a height of 2–7 cm), the system recorded 85 events, corresponding to a response accuracy of 85%.

The dynamics of noise interference under a normal mode and in the presence of external influences are clearly demonstrated in Fig. 20, 21. The false alarm rate did not exceed 15%, demonstrating the high noise immunity of The designed system. In the absence of mechanical load, the system interface remains completely black (Fig. 15), further confirming the effectiveness and reliability of the noise compensation algorithms. Our results demonstrate that the proposed system is capable of reliably distinguishing the useful signal from background interference, ensuring stable operation under real-world operating conditions.

The results demonstrate that the designed laboratory ATCMS prototype possesses sufficient sensitivity, accuracy, and noise immunity for continuous monitoring of fiber-optic communication lines up to 60 km long. Switching to wavelengths of 750–850 nm and further improvement of the AI algorithms will increase the monitoring range and improve the accuracy of classifying types of influences.

The limitations of this study are primarily related to the use of a 650 nm wavelength, which is characterized by increased optical loss in single-mode G.652 fiber. This limits the maximum length of the monitored sections, which in the experiments conducted does not exceed 60 km. Furthermore, the results are reproducible within the specified range of mechanical stresses and strain rates used under laboratory conditions, which requires additional verification when expanding the range of input parameters and moving on to field testing.

Disadvantages of our study include the sensitivity of measurements to laser source noise and external vibration, as well as the dependence of recording accuracy on the resolution of the image sensor used. These caveats do not limit the fundamental functionality of the system but may lead to increased error under weak stresses. These limitations can be further mitigated by stabilizing the radiation source, using adaptive noise filtering algorithms, as well as applying image sensors with improved sensitivity characteristics.

Further research could focus on switching to wavelengths of 750–850 nm to increase the length of monitored lines, implementing machine learning methods for automatically classifying impact types, and expanding the system to multi-channel quasi-distributed monitoring. However, the main challenges may include construction of mathematical models for interpreting complex optical patterns, ensuring the stability of processing algorithms under changing external conditions, and conducting large-scale experimental tests under real-world operating conditions. Future field tests at existing facilities are recommended to verify interference immunity under real-world operating conditions (temperature fluctuations, vehicle vibration, electromagnetic fields), as well as developing machine learning algorithms to categorize impact types and reduce the likelihood of false alarms.

7. Conclusions

1. We have scientifically substantiated the principle for monitoring the technical condition of fiber-optic cables based on recording and intelligent optical-digital analysis of changes in the pixel structure of the optical spot formed by cladding radiation when the fiber undergoes microbending under mechanical stress. This principle differs from conventional interferometric and reflectometric methods by eliminating the analysis of the primary wave in the core and switching to processing of secondary cladding radiation, which significantly reduces system cost, facilitates ease of implementation, and provides high immunity to external interference.

2. The designed hardware and software system successfully implements high-frequency image capture of the light spot (up to hundreds of frames per second), positive-to-negative image conversion with the exclusion of the fiber core from analysis, numerical pixel counting in informative areas of the cladding, and intelligent noise filtering, enabling real-time detection of additional optical losses caused by mechanical stress on the fiber cable. Mathematical modeling and experimental studies confirmed a linear correlation between changes in the pixel structure of the optical spot and the magnitude of the applied load causing microbending of the fiber. These results are explained by the photoelastic effect and the redistribution of optical power between the fiber core and cladding.

3. The designed laboratory prototype of ATCMS, based on standard single-mode ITU-T G.652.D fiber optic cable, a 650 nm laser source, and inexpensive CMOS image sensors with a resolution of up to Full HD (1920×1080, 2,073,600 pixels), enables stable formation and recording of a light spot sensitive to microbending and deformation of the fiber optic cable. This confirms the feasibility of designing a low-cost monitoring system using mass-produced components. This technological advancement can serve as the basis for a method for continuously monitoring the integrity of fiber optic data transmission lines, including the detection of mechanical impacts and potential unauthorized access. The demonstrated immunity to interference (no false alarms under laboratory conditions) and high sensitivity to loads from 5 N confirm the potential for scaling the system for real-world communication lines up to 60 km long.

4. An assessment of sensitivity, interference immunity, response accuracy, and the correlation of optical spot parameters with mechanical impact types was conducted under laboratory conditions. A 10 mm diameter cable in a plastic sheath was placed on a wooden surface, and 100 different impacts (light impacts and pressures from 5 N) were applied. The system recorded 80 events, demonstrating sensitivity from 5 N, response accuracy of 80%, and a linear correlation between the spot area and the level of optical loss. Interference immunity was confirmed by the absence of false alarms in control tests without impact.

Conflicts of interest

The authors declare that they have no conflicts of interest in relation to the current study, including financial, personal, authorship, or any other, that could affect the study, as well as the results reported in this paper.

Data availability

The data will be provided upon reasonable request.

Use of artificial intelligence

The authors confirm that they did not use artificial intelligence technologies when creating the current work.

Authors' contributions

Aliya Alkina: Methodology, Data curation, Formal analysis, Resources, Validation, Writing – review & editing; **Ali Mekhtiyev**: Conceptualization, Methodology, Formal analysis, Investigation, Data curation, Writing – original draft, Writing – review & editing; **Yelena Neshina**: Concep-

tualization, Project administration, Supervision, Resources, Validation, Writing – review & editing, Correspondence; **Adam Ujma**: Formal analysis, Investigation, Methodology, Writing – original draft; **Ruslan Mekhtiyev**: Software, Formal analysis, Visualization; **Madiyar Musagazhinov**: Software, Visualization, Data curation; **Yekaterina Bilichenko**: Methodology, Formal analysis, Validation, Writing – review & editing.

References

1. Guemes, A., Mujica, L. E., del-Río-Velilla, D., Fernandez-Lopez, A. (2025). Structural Health Monitoring by Fiber Optic Sensors. Photonics, 12 (6), 604. https://doi.org/10.3390/photonics12060604
2. Bado, M. F., Casas, J. R. (2021). A Review of Recent Distributed Optical Fiber Sensors Applications for Civil Engineering Structural Health Monitoring. Sensors, 21 (5), 1818. https://doi.org/10.3390/s21051818
3. Wang, W., Yiu, H. H. P., Li, W. J., Roy, V. A. L. (2021). The Principle and Architectures of Optical Stress Sensors and the Progress on the Development of Microbend Optical Sensors. Advanced Optical Materials, 9 (10). https://doi.org/10.1002/adom.202001693
4. Zhang, X., Zhu, H., Jiang, X., Broere, W. (2024). Distributed fiber optic sensors for tunnel monitoring: A state-of-the-art review. Journal of Rock Mechanics and Geotechnical Engineering, 16 (9), 3841–3863. https://doi.org/10.1016/j.jrmge.2024.01.008
5. Wang, Z., Lu, B., Ye, Q., Cai, H. (2020). Recent Progress in Distributed Fiber Acoustic Sensing with Φ-OTDR. Sensors, 20 (22), 6594. https://doi.org/10.3390/s20226594
6. Chapalo, I., Stylianou, A., Mégret, P., Theodosiou, A. (2024). Advances in Optical Fiber Speckle Sensing: A Comprehensive Review. Photonics, 11 (4), 299. https://doi.org/10.3390/photonics11040299
7. Cao, L., Abedin, S., Cui, G., Wang, X. (2025). Artificial Intelligence and Machine Learning in Optical Fiber Sensors: A Review. Sensors, 25 (24), 7442. https://doi.org/10.3390/s25247442
8. Hu, X., Bai, X., Li, J., He, Y., Li, Y., Li, L. et al. (2025). A fiber optic sensing intrusion detection method based on WPD-EMD and improved ResNet. Optical Fiber Technology, 90, 104125. https://doi.org/10.1016/j.yofte.2024.104125
9. Peng, F., Wu, H., Jia, X.-H., Rao, Y.-J., Wang, Z.-N., Peng, Z.-P. (2014). Ultra-long high-sensitivity Φ-OTDR for high spatial resolution intrusion detection of pipelines. Optics Express, 22 (11), 13804. https://doi.org/10.1364/oe.22.013804
10. Xu, S., Qin, Z., Zhang, W., Xiong, X. (2020). Monitoring Vehicles on Highway by Dual-Channel φ-OTDR. Applied Sciences, 10 (5), 1839. https://doi.org/10.3390/app10051839
11. Hu, X., Qiu, G., Karimi, H. R., Zhang, D. (2024). TFF-CNN: Distributed optical fiber sensing intrusion detection framework based on two-dimensional multi-features. Neurocomputing, 564, 126959. https://doi.org/10.1016/j.neucom.2023.126959
12. Yang, N., Zhao, Y., Chen, J. (2022). Real-Time Φ-OTDR Vibration Event Recognition Based on Image Target Detection. Sensors, 22 (3), 1127. https://doi.org/10.3390/s22031127
13. Zhang, S., Xie, S., Li, Y., Yuan, M., Qian, X. (2023). Detection of Gas Pipeline Leakage Using Distributed Optical Fiber Sensors: Multi-Physics Analysis of Leakage-Fiber Coupling Mechanism in Soil Environment. Sensors, 23 (12), 5430. https://doi.org/10.3390/s23125430
14. Fabbricatore, F., Bertola, N. (2005). Structural performance monitoring for concrete girder bridges with distributed fiber optic sensors. 13th International Conference on Structural Health Monitoring of Intelligent Infrastructure. https://doi.org/10.3217/978-3-99161-057-1-022
15. Tan, X., Poorghasem, S., Huang, Y., Feng, X., Bao, Y. (2024). Monitoring of pipelines subjected to interactive bending and dent using distributed fiber optic sensors. Automation in Construction, 160, 105306. https://doi.org/10.1016/j.autcon.2024.105306
16. Abdallah, A., Fouad, M. M., Ahmed, H. N. (2021). Low-cost real-time fiber optic sensor for intrusion detection. Sensor Review, 42 (1), 89–101. https://doi.org/10.1108/sr-03-2021-0090
17. Mekhtiyev, A., Dunayev, P., Neshina, Y., Alkina, A., Aimagambetova, R., Mukhambetov, G. et al. (2023). Power supply via fiber-optical conductor for sensors of mine working monitoring system. Eastern-European Journal of Enterprise Technologies, 5 (5 (125)), 15–23. https://doi.org/10.15587/1729-4061.2023.289775
18. Yugay, V., Mekhtiyev, A., Neshina, Y., Aubakirova, B., Aimagambetova, R., Kozhas, A. et al. (2021). Design of an information-measuring system for monitoring deformation and displacement of rock massif layers based on fiber-optic sensors. Eastern-European Journal of Enterprise Technologies, 6 (5 (114)), 12–27. https://doi.org/10.15587/1729-4061.2021.244897
19. Yugay, V., Mekhtiyev, A., Madi, P., Neshina, Y., Alkina, A., Gazizov, F. et al. (2022). Fiber-Optic System for Monitoring Pressure Changes on Mine Support Elements. Sensors, 22 (5), 1735. https://doi.org/10.3390/s22051735
20. Mekhtiyev, A., Neshina, Y., Alkina, A., Yugay, V., Kalytka, V., Sarsikeyev, Y., Kirichenko, L. (2023). Developing an Intelligent Fiber-Optic System for Monitoring Reinforced Concrete Foundation Structure Damage. Applied Sciences, 13 (21), 11987. https://doi.org/10.3390/app132111987
21. Yang, X., Qiu, J., Gong, X., Ye, J., Yao, F., Chen, J. et al. (2025). Anomaly Diagnosis Using Machine Learning Method in Fiber Fault Diagnosis. Computers, Materials & Continua, 85 (1), 1515–1539. https://doi.org/10.32604/cmc.2025.067518